Journal of the American Heart Association

ORIGINAL RESEARCH

Role of PARP and TRPM2 in VEGF Inhibitor-Induced Vascular Dysfunction

Karla B. Neves, PhD; Rheure Alves-Lopes, PhD; Augusto C. Montezano, PhD; Rhian M. Touyz, MD, PhD

BACKGROUND: Hypertension and vascular toxicity are major unwanted side effects of antiangiogenic drugs, such as vascular endothelial growth factor inhibitors (VEGFis), which are effective anticancer drugs but have unwanted side effects, including vascular toxicity and hypertension. Poly (ADP-ribose) polymerase (PARP) inhibitors, used to treat ovarian and other cancers, have also been associated with elevated blood pressure. However, when patients with cancer receive both olaparib, a PARP inhibitor, and VEGFi, the risk of blood pressure elevation is reduced. Underlying molecular mechanisms are unclear, but PARP-regulated transient receptor potential cation channel, subfamily M, member 2 (TRPM2), a redox-sensitive calcium channel, may be important. We investigated whether PARP/TRPM2 plays a role in VEGFi-induced vascular dysfunction and whether PARP inhibition ameliorates the vasculopathy associated with VEGF inhibition.

METHODS AND RESULTS: Human vascular smooth muscle cells (VSMCs), human aortic endothelial cells, and wild-type mouse mesenteric arteries were studied. Cells/arteries were exposed to axitinib (VEGFi) alone and in combination with olaparib. Reactive oxygen species production, Ca^{2+} influx, protein/gene analysis, PARP activity, and TRPM2 signaling were assessed in VSMCs, and nitric oxide levels were determined in endothelial cells. Vascular function was assessed by myography. Axitinib increased PARP activity in VSMCs in a reactive oxygen species-dependent manner. Endothelial dysfunction and hypercontractile responses were ameliorated by olaparib and a TRPM2 blocker (8-Br-cADPR). VSMC reactive oxygen species production, Ca^{2+} influx, and phosphorylation of myosin light chain 20 and endothelial nitric oxide synthase (Thr^{495}) were augmented by axitinib and attenuated by olaparib and TRPM2 inhibition. Proinflammatory markers were upregulated in axitinib-stimulated VSMCs, which was reduced by reactive oxygen species scavengers and PARP-TRPM2 inhibition. Human aortic endothelial cells exposed to combined olaparib and axitinib showed nitric oxide levels similar to VEGF-stimulated cells.

CONCLUSIONS: Axitinib-mediated vascular dysfunction involves PARP and TRPM2, which, when inhibited, ameliorate the injurious effects of VEGFi. Our findings define a potential mechanism whereby PARP inhibitor may attenuate vascular toxicity in VEGFi-treated patients with cancer.

Key Words: PARP ■ TRPM2 ■ vascular dysfunction ■ VEGF

Over the past decade, survival of patients with cancer has improved substantially because of the development of new therapeutic strategies. Angiogenesis inhibitors, including vascular endothelial growth factor (VEGF) inhibitors (VEGFis), have revolutionized anticancer treatment for a wide range of malignancies.[1,2] VEGF is secreted by various cell types, including endothelial cells, fibroblasts, and tumor cells, and plays a crucial role in angiogenesis, the formation of new blood vessels from preexisting vessels, which is vital for the growth and spread of solid tumors. VEGFis, by inhibiting angiogenesis, have markedly improved outcomes in various cancers such as metastatic renal carcinoma, advanced hepatocellular carcinoma, cervical cancer, and gastrointestinal stroma cell tumors.[1–3] Despite these benefits, VEGFis are associated with unwanted side effects, especially cardiovascular toxicities including hypertension, left ventricular systolic dysfunction and heart failure, and

Correspondence to: Rhian M. Touyz, MD, PhD, Research Institute of McGill University Health Centre, 1001 Decarie Boulevard, Montreal H4A 3J1, Canada. Email: rhian.touyz@mcgill.caKarla B. Neves, PhD, Strathclyde Institute of Pharmacy and Biomedical Sciences, University of Strathclyde, 161 Cathedral Street, Glasgow, G4 0RE, United Kingdom. Email: karla.neves@strath.ac.uk

Supplemental Material is available at https://www.ahajournals.org/doi/suppl/10.1161/JAHA.122.027769

For Sources of Funding and Disclosures, see page 12.

JAHA is available at: www.ahajournals.org/journal/jaha

CLINICAL PERSPECTIVE

What Is New?

- We identify poly (ADP-ribose) polymerase/transient receptor potential cation channel, subfamily M, member 2 as a novel pathway underlying vascular smooth muscle cell toxicity and vascular dysfunction induced by vascular endothelial growth factor (VEGF) inhibition.
- Inhibition of poly (ADP-ribose) polymerase/transient receptor potential cation channel, subfamily M, member 2 ameliorated VEGF inhibitor–induced vascular effects suggest a vasoprotective effect.

What Are the Clinical Implications?

- VEGF inhibitor–induced hypertension may be less common in patients with cancer cotreated with olaparib.
- Molecular mechanisms underlying the possible beneficial vascular effects of olaparib during VEGF inhibitor anticancer therapy remain unclear.
- We define a putative vasoprotective effect of olaparib involving transient receptor potential cation channel, subfamily M, member 2 that may ameliorate vascular injury induced by VEGF inhibitors in cancer treatment, which has important clinical implications because combination therapy with poly (ADP-ribose) polymerase–VEGF inhibition improves cancer survival and may also reduce risk of vascular toxicity and hypertension; however, this awaits confirmation.

Nonstandard Abbreviations and Acronyms

eNOS	endothelial nitric oxide synthase
HAEC	human aortic endothelial cells
NO	nitric oxide
PARP	poly (ADP-ribose) polymerase
PARPi	poly (ADP-ribose) polymerase inhibitor
ROS	reactive oxygen species
TRPM2	transient receptor potential cation channel, subfamily M, member 2
VEGFi	vascular endothelial growth factor inhibitor
VSMC	vascular smooth muscle cell

arterial and venous thromboembolism. Systemic hypertension is the most common comorbidity among patients with cancer treated with VEGFis and is the major cause of increased risk for developing adverse cardiovascular events.[1,4,5] However, molecular mechanisms underlying the increase in blood pressure in VEGFi-treated patients are still not fully elucidated.

Recent studies have explored the possibility that VEGFis in combination with other, newer anticancer drugs may have added anticancer effects.[6] In particular, there is growing interest in the therapeutic potential of VEGFis with poly (ADP-ribose) polymerase (PARP) inhibitors (PARPis). PARPis prevent repair of DNA in cancer cells, causing cell death. Several PARPis have been approved for the treatment of *BRCA*-mutated ovarian, breast, and pancreatic cancer, and many clinical trials are still ongoing.[6,7] A phase 3 trial demonstrated significant progression-free survival when patients with advanced ovarian cancer were treated with both bevacizumab and olaparib.[8] An interesting observation was that the number of patients with hypertension was in the combination therapy group than in the group treated only with VEGFis.[8] These findings suggest that there may be interplay between PARP and VEGF signaling pathways that may influence vascular function.

PARP, when activated, attaches ADP-ribose polymer chains to target proteins and uses nicotinamide adenine dinucleotide as a substrate, thereby facilitating DNA repair. PARP also has other functions, including stress signaling, cell differentiation, inflammation, and vascular calcification. A critical regulator of PARP is reactive oxygen species (ROS), which, together with ADP-ribose, influence activation of transient receptor potential cation channel, subfamily M, member 2 (TRPM2).[9–11] TRPM2 is a highly redox-sensitive Ca^{2+} channel that is associated with hypertension-induced vascular dysfunction.[12,13] PARP inhibition is vasoprotective in various disease models. In experimental models of hypertension and diabetes, PARPis improved endothelial dysfunction, prevented cardiomyocyte necrosis, and reduced myocardial infarction size after cardiac reperfusion injury.[14,15] Some of these effects likely involve TRPM2.[9]

Considering the growing evidence that PARP and redox-sensitive TRPM2 are important players in vascular cells, and that VEGFis induce vascular injury through ROS, as we previously demonstrated,[16] we sought to examine whether there is interplay between PARP, TRPM2, and VEGF and if VEGFi-induced vascular dysfunction involves PARP/TRPM2.

METHODS

The data that support the findings of this study are available from the corresponding author on reasonable request.

Study Approval

Ethics approval for the use of human blood vessel samples was obtained from the West of Scotland Research

Ethics Service (WS/12/0294). Written informed consent was obtained for all study participants in accordance with the Declaration of Helsinki. Experiments were approved by the University of Glasgow Animal Welfare and Ethics Review Board. All experimental protocols on mice were performed in accordance with the United Kingdom Animals Scientific Procedures Act 1986 (License No. 70/9021) and with Animal Research: Reporting of In Vivo Experiments Guidelines.

Vascular Function Studies

Mouse mesenteric resistance arteries (first and second order; 300–350 μm) were isolated from male and female wild type mice (FVB background) at 10 to 12 weeks of age (20–25 g). Briefly, arterial segments were mounted on isometric wire myographs (Danish Myo Technology, Denmark) filled with 5 mL of physiological saline solution (in mmol/L: 130 NaCl, 14.9 $NaHCO_3$, 4.7 KCl, 1.18KH_2PO_4, 1.17 $MgSO_4 \cdot 7H_2O$, 5.5 glucose, 1.56 $CaCl_2 \cdot 2H_2O$, and 0.026 EDTA) and continuously gassed with a mixture of 95% O_2 and 5% CO_2 while being maintained at a constant temperature of 37±0.5 °C. Following 30 minutes of equilibration, the contractile responses of arterial segments were assessed by the addition of KCl (62.5 mmol/L). The integrity of the endothelium was verified by relaxation induced by acetylcholine (1 μmol/L) in arteries precontracted with thromboxane A2 agonist (U46619; 0.1 μmol/L). Endothelium-dependent relaxation was assessed as a dose–response to acetylcholine (10^{-9}–3×10^{-5} mol/L). Endothelium-independent vasorelaxation was assessed by a dose–response to sodium nitroprusside (10^{-10}–3×10^{-5} mol/L). Concentration–response curves to U46619 (10^{-10}–10^{-6} mol/L) and endothelin-1 (ET-1; 10^{-12}–3×10^{-7} mol/L) were performed to evaluate vasoconstriction. Vascular functional responses were assessed in the presence of axitinib (VEGFi, 1 μmol/L, 30 minutes) with and without olaparib (PARPi; 1 μmol/L, 30 minutes) or 8-Br-cADPR (8-Br; a cyclic ADP-ribose inhibitor, which consequently inhibits TRPM2 activation; 1 μmol/L, 30 minutes). The number of animals used is highlihted in the figure legends for each experiment.

Vascular Smooth Muscle Cell Isolation

Primary vascular smooth muscle cells (VSMCs) were isolated from small arteries obtained from healthy patients undergoing elective maxillofacial surgery at the Craniofacial/Oral and Maxillofacial Unit, Queen Elizabeth University Hospital, Glasgow, by enzymatic digestion, as we previously described.[17] Briefly, cleaned arteries were placed in Ham's F-12 culture medium containing 1% gentamicin, collagenase (type 1), elastase, soybean trypsin inhibitor, and BSA, and were incubated for 30 to 60 minutes at 37 °C under constant agitation. The digested tissue was further dissociated by repeated aspiration through a syringe with a 20G needle. The cell suspension was centrifuged (500 *g*, 4 minutes), and the cell pellet was resuspended in Ham's F-12 culture medium containing 10% FBS. Cells were seeded onto 25 mm flask. VSMCs were maintained in DMEM media supplemented with 10%FBS and penicillin/streptomycin (50 μg/mL). Before experimentation, cells were rendered quiescent by maintenance in a reduced growth supplement medium (0.5% FBS) overnight. Only primary, low-passage cells (passages 4–8) were studied. Cells were exposed to axitinib (1 μmol/L) in the presence or absence of pharmacological inhibitors (olaparib, 1 μmol/L; 8-Br-cADPR, 1 μmol/L or Tiron [ROS scavenger], 10 μmol/L) for different time points.

Human Aortic Endothelial Cells

For cell-based studies in endothelial cells, we used human aortic endothelial cells (HAECs; ATCC, Middlesex, UK; PCS-100-011). HAECs were cultured in Endothelial Cell Growth Medium (PromoCell, Heidelberg, Germany) supplemented with penicillin/streptomycin (50 μg/mL) and Endothelial Cell Growth Medium Supplement (10 mL; Promocell). For functional studies, confluent cells were made quiescent for 2 hours in low-serum medium containing 0.5% FBS and stimulated with total VEGF (20 ng/mL), axitinib, and the combination axitinib + olaparib as described above.

Lucigenin-Enhanced Chemiluminescence

Lucigenin-derived chemiluminescence assay was used to determine NADPH-dependent ROS production in human VSMC homogenates as we previously described.[18] Briefly, cells were homogenized in lysis buffer (20 mmol/L of KH_2PO_4, 1 mmol/L of EGTA, 1 μg/mL of aprotinin, 1 μg/mL of leupeptin, 1 μg/mL of pepstatin, and 1 mmol/L of PMSF). 50 μL of the sample were added to a suspension containing 175 μL of assay buffer (50 mmol/L of KH_2PO_4, 1 mmol/L of EGTA, and 150 mmol/L of sucrose) and lucigenin (5 μmol/L). Luminescence was measured with a luminometer (AutoLumat LB 953, Berthold, Bad Wildbad, Germany) before and after stimulation with NADPH (100 μmoL/L). A buffer blank was subtracted from each reading. Results were normalized by concentration of protein, as measured by the BCA assay.

Amplex Red Assay

The H_2O_2 levels were measured by Amplex red assay in human VSMCs. Protocols followed the manufacturer's instructions using the horseradish peroxidase linked amplex red fluorescence assay (A22188; Life Technologies, Carlsbad, CA). Fluorescence readings were made in a

96-well plate at Ex/Em=530/590 nm. H_2O_2 production was normalized to protein concentration.

Electron Paramagnetic Resonance

Human VSMC O_2^- production was measured by electron paramagnetic resonance. Electron paramagnetic resonance samples were placed in 50-μL glass capillaries, and measurements were performed by Bruker BioSpin's (Billerica, MA) e-scan electron paramagnetic resonance equipped with a super-high Q microwave cavity at room temperature using *CMH* hydrochloride spin probe (Enzo Life Sciences, Exeter, UK). The electron paramagnetic resonance instrument settings for experiments with membrane fractions were as follows: field sweep, 50 G; microwave frequency, 9.78 GHz; microwave power, 20 mW; modulation amplitude, 2 G; conversion time, 656 milliseconds; time constant, 656 milliseconds; and 512 points resolution and receiver gain, 1×10^5. Results were normalized to protein concentration.

Real-Time Polymerase Chain Reaction

Real-time polymerase chain reaction (Qiagen, Manchester, UK) was used to assess mRNA expression in human VSMCs. Briefly, total RNA was extracted using TRIzol (Qiagen), treated with RNase-free DNAse I, and 2 μg of RNA was reverse transcribed in a reaction containing 100 μg/mL oligo-dT, 10 mmol/L of 2′-deoxynucleoside 5′-triphosphate, 5×first-Strand buffer, and 2 μL of 200-U reverse transcriptase. For real-time polymerase chain reaction amplification, 3 μL of each reverse transcription product were diluted in a reaction buffer containing 5 μL of SYBR Green polymerase chain reaction master mix and 300 nmol/L of primers in a final volume of 10 μL per sample. The reaction conditions consisted of 2 steps at 50 °C for 2 minutes and 95 °C for 2 minutes, followed by 40 cycles of 3 steps, 15-second denaturation at 95 °C, 60-second annealing at 60 °C, and 15 seconds at 72 °C. Human primers used are detailed in Table S1. Data are expressed as target gene/GAPDH housekeeping gene. Relative gene expression was calculated using the $2^{\Delta\Delta Ct}$ method.

Measurement of Intracellular Ca^{2+} Transients in VSMCs

VSMC Ca^{2+} signaling was assessed using the fluorescent Ca^{2+} indicator, Cal-520 acetoxymethyl ester (Cal-520/AM; 10 μmol/L; Abcam, Cambridge, UK). Cells were grown in 12-well plates and following removal of culture media were incubated with Cal-520 AM in 0.5% FBS at 37 °C for 75 minutes followed by 30 minutes at room temperature. Following incubation, the dye solution was replaced with HEPES physiological saline solution (1.3×10^{-1} mol/L NaCl, 5×10^{-3} mol/L KCl, 10^{-3} mol/L CaCl, 10^{-3} mol/L MgCl, 2×10^{-2} mol/L HEPES, and 10^{-2} mol/L D-glucose, pH 7.4) for 30 minutes prior to imaging. Fluorescence intensity as a measure of $[Ca^{2+}]_i$, was monitored for 30 seconds in basal condition and 180 minutes under endothelin-1 (0.1 μmol/L) or U46619 (1 μmol/L) stimulation. In some experiments, VSMCs were pretreated for 30 minutes with olaparib (1 μmol/L) or 8-Br-cADPR (1 μmol/L). Fluorescence-based measurements of Ca^{2+} signals were performed using an inverted epifluorescence microscope (Axio Observer Z1 Live-Cell imaging system; Zeiss, Cambridge, UK) with excitation/emission wavelengths 490/535 nm, respectively. Images were acquired and analyzed using the Zen Blue Program (Zeiss, Cambridge, UK).

Immunoblotting

Protein was extracted from human VSMCs or aorta isolated from FVB mice. Protein (20–30 μg) was separated by electrophoresis on a polyacrylamide gel and transferred to a nitrocellulose membrane. Nonspecific binding sites were blocked with 3% BSA in Tris-buffered saline solution. Membranes were then incubated with specific antibodies overnight at 4 °C. Membranes were washed 3 times with Tris-buffered saline–Tween20 and incubated with infrared dye–labeled secondary antibodies for 1 hour at room temperature. Membranes were visualized using an Odyssey CLx infrared imaging system (Li-Cor Biosciences UK Ltd, Cambridge, UK), and results were normalized to the total form of the protein or α-tubulin and are expressed in arbitrary units compared with vehicle group. Antibodies used were as follows: anti–α-tubulin (1:5000, ab4074; Abcam); anti–phospho- myosin light chain 20 (MLC20) (1:1000, ab89594; Abcam), anti–total MLC20 (1:1000, ab137550; Abcam), anti–phospho-endothelial nitric oxide synthase (eNOS)^{Thr495} (1:500; Santa Cruz, UK); anti-phospho-eNOS^{Ser1177} (1:1000; Cell Signaling Technology, Leiden, UK); anti-total-eNOS (1:1000; Cell Signaling Technology); anti–NF-κB (1:500; Cell Signaling Technology); and anti-β-actin (1:10000; Sigma, Hertfordshire, UK).

Nitric Oxide Production

Production of nitric oxide (NO) was determined using the NO fluorescent probe diacetate 4-amino-5-methylamino-2′,7′-difluorofluorescein diacetate (Life Technologies, Molecular Probes, Paisley, UK). HAECs were loaded with diacetate 4-amino-5-methylamino-2′,7′-difluorofluorescein (final concentration 5 μmol/L, 30 minutes) in serum free media, kept in the dark, and maintained at 37 °C, as we previously described.[19] Briefly, cells were washed to remove exceeding probe. Medium was replaced and incubated for an additional

10 minutes to allow complete de-esterification of the intracellular diacetates. Cells were stimulated following experimental protocol. Cells were washed with PBS and harvested with mild trypsinization at 0.025%. Trypsin was inactivated with soybean trypsin inhibitor (0.025%) in PBS (1:1). After washing, the pellet was transferred to a black 96 well microplate (BD Falcon, Loughborough, UK). The diacetate 4-amino-5-met hylamino-2′,7′-difluorofluorescein fluorescence was assessed with a spectrofluorometer at excitation/emission wavelengths of 495/515 nm. Fluorescence intensity was normalized to the protein concentration and expressed as fluorescence emission/μg of protein.

Small Interfering RNA Transfection

Human VSMCs were transiently transfected with 100 nmol/L with ON-TARGET plus Human TRPM2 (7226) small interfering RNA (siRNA)—SMARTpool from Dharmacon (L-004193-00-0050) for 7 hours. For housekeeping, GAPDH siRNA was used (D-001830-10-20 - Dharmacon). As a control, we used ON-TARGETplus Non-targeting Control Pool from Dharmacon (D-001810–10-20). Experiments were performed at 48 hours after transfections. Transfection efficiency was measured by real-time western blotting.

ELISA

Interleukin-1β, interleukin-6, and monocyte chemoattractant protein 1 levels were detected in this study in human VSMC media by ELISA according to the manufacturer's protocol (DY201, DY206, and DY279, respectively, R&D Systems, Abingdon, UK).

PARP Colorimetric Assay

PARP activity was assessed on the basis of the detection of biotinylated poly (ADP-ribose) deposited by

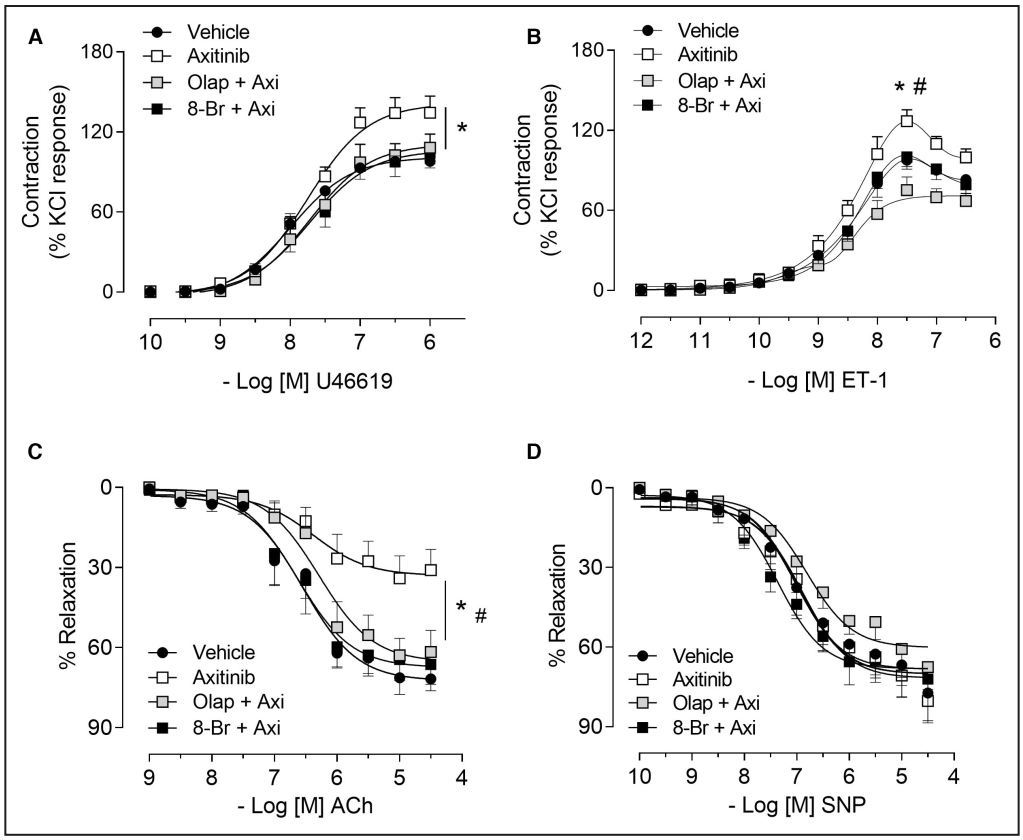

Figure 1. Axitinib induces vascular dysfunction via poly (ADP-ribose) polymerase (PARP) and transient receptor potential cation channel, subfamily M, member 2 (TRPM2).
Vascular functional responses in mesenteric arteries obtained from wildtype mice in response to U46619 (**A**), endothelin-1 (ET-1) (**B**), acetylcholine (ACh) and sodium nitroprusside (SNP) (**C**). Vessels were mounted on wire myograph. The increase in contraction and impaired relaxation induced by axitinib was ameliorated in vessels pretreated with the PARP inhibitor olaparib and TRPM2 inhibitor 8-Br-cADPR (**A**–**C**). Curves represent the mean±SEM. For ACh and SNP, responses were expressed as percentage of U46619-induced preconstriction (n=4–9/group). The Kruskal–Wallis nonparametric test showed for U46619 **P*<0.05 axitinib vs vehicle; ET-1 and ACh: **P*<0.05 axtinib vs vehicle, # Olap+Axi and 8-Br+Axi vs axitinib.

PARP-1 onto immobilized histones in human VSMCs exposed to axitinib in presence and absence of pharmacological inhibitors by a colorimetric assay according to the manufacturer's protocol (4677-096-K, R&D Systems). Results were normalized to the protein concentration.

Statistical Analysis

For vascular functional studies, data were analyzed by determining EC_{50} and maximal response values from experimental data fitted to a 4-parameter logistic function against the null hypothesis. pD_2 (defined as the negative logarithm of the EC_{50} values) and maximal response were compared by 2-way ANOVA with Bonferroni posttest, as appropriate. For the other experiments, statistical comparisons between groups were performed using two-tailed Student's *t*-test and or one-way ANOVA. Bonferroni or Dunnett posttest was used as appropriate. $P<0.05$ was considered statistically significant. Data analysis was conducted using Prism version 8.0 (GraphPad Software Inc., San Diego, CA). Data are expressed as mean±SEM.

RESULTS

Vascular Dysfunction Induced by Axitinib Involves PARP and TRPM2

We assessed vascular reactivity in resistance arteries from mice exposed acutely to axitinib, and demonstrated that this VEGFi augmented the contractile response induced by U46619 and endothelin-1 ($P<0.05$). In vessels preexposed to olaparib and 8-Br-cADPR hypercontractile responses to axitinib were attenuated (Figure 1A, 1B).

Axitinib blunted acetylcholine-induced vasodilation ($P<0.001$). These effects were blocked by olaparib and 8-Br-cADPR (Figure 1C). No changes were observed in sodium nitroprusside–induced relaxation (Figure 1D). To determine whether olaparib effects are drug specific or generalized responses to PARP inhibition, we also studied niraparib, another PARPi. As shown in Figure S1A and S1B, niraparib attenuated axitinib-induced vascular contraction ($P<0.05$) and normalized acetylcholine-mediated endothelial dysfunction ($P<0.0001$) similar to olaparib (Figure S1C).

Axitinib Increases ROS Production, PARP Activity, and TRPM2 Expression in VSMCs

To explore possible molecular mechanisms linking VEGF, PARP, and redox signaling, we evaluated effects of axitinib on VSMC production of superoxide (O_2^-) and H_2O_2, PARP activity, and TRPM2 expression. As shown in Figure 2, axitinib increased NADPH-dependent ROS production and stimulated an increase in O_2^- generation in a time-dependent manner ($P<0.05$; Figure 2A, 2B). On the other hand, axitinib stimulation resulted in a rapid decrease in H_2O_2 levels ($P<0.01$; Figure 2C). Increased ROS levels were associated with greater PARP activity in VSMC exposed to axitinib, which was blocked by olaparib and tiron (ROS scavenger; $P<0.001$; Figure 2D). These phenomena were associated with an increase in TRPM2 mRNA expression ($P<0.05$), which was attenuated by PARP inhibition ($P<0.001$; Figure 2E).

PARP and TRPM2 Inhibition Attenuate Axitinib-Induced Procontractile Signaling

VSMC contraction is triggered by an increase in intracellular free Ca^{2+} concentration and activation of procontractile signaling molecules including myosin light chain.[20] Molecular studies showed that axitinib enhances Ca^{2+} influx induced by endothelin-1 ($P<0.001$; Figure 3A) and U46619 ($P<0.05$; Figure S2A) in VSMCs, which was dependent on PARP-TRPM2 activation as this was blocked by olaparib and 8-Br-cADPR (Figure 3A, Figure S2A). The role of TRPM2 on axitinib-induced Ca^{2+} transients was confirmed by TRPM2 silencing in VSMCs. Cells exposed to TRPM2 siRNA no longer showed an increase in Ca^{2+} influx in response to endothelin-1 ($P<0.001$; Figure 3B) or U46619 ($P=0.05$; Figure S2B) when incubated with axitinib.

Axitinib increased phosphorylation of the contractile marker MLC20 in human VSMCs ($P<0.05$; Figure 3C) and mouse aorta ($P<0.05$; Figure S3B). This response was blocked by PARP inhibition (Figure 3C) and TRMP2 siRNA ($P<0.05$; Figure 3D). Corroborating our previous data, we also showed that the ROS scavenger tiron decreased axitinib-induced MLC20 phosphorylation in human VSMCs (Figure S3A; $P<0.05$).

Proinflammatory Effects of Axitinib Are Blunted by Inhibition of PARP and TRPM2

Evidence suggests that activation of the TRPM2 channel leads to generation of proinflammatory cytokines, and consequently causes inflammation and tissue damage.[21] We demonstrated that axitinib increases mRNA expression of interleukin-1β, interleukin-6, and monocyte chemoattractant protein 1 in human VSMCs (Figure 4A, 4C, 4E; $P<0.05$). This was associated with increased production of these cytokines as evidenced by increased levels in the culture media (Figure 4B, 4D, 4F; $P<0.05$). Pretreatment of VSMCs with olaparib, 8-Br-cADPR, and tiron prevented axitinib-stimulated cytokine production (Figure 4; $P<0.05$). Inducible NO synthase mRNA levels and NF-κB protein expression were also increased by axitinib in human VSMCs ($P<0.001$), which was inhibited by olaparib ($P<0.001$ and $P<0.05$, respectively) and tiron ($P<0.05$; Figures S4 and S5).

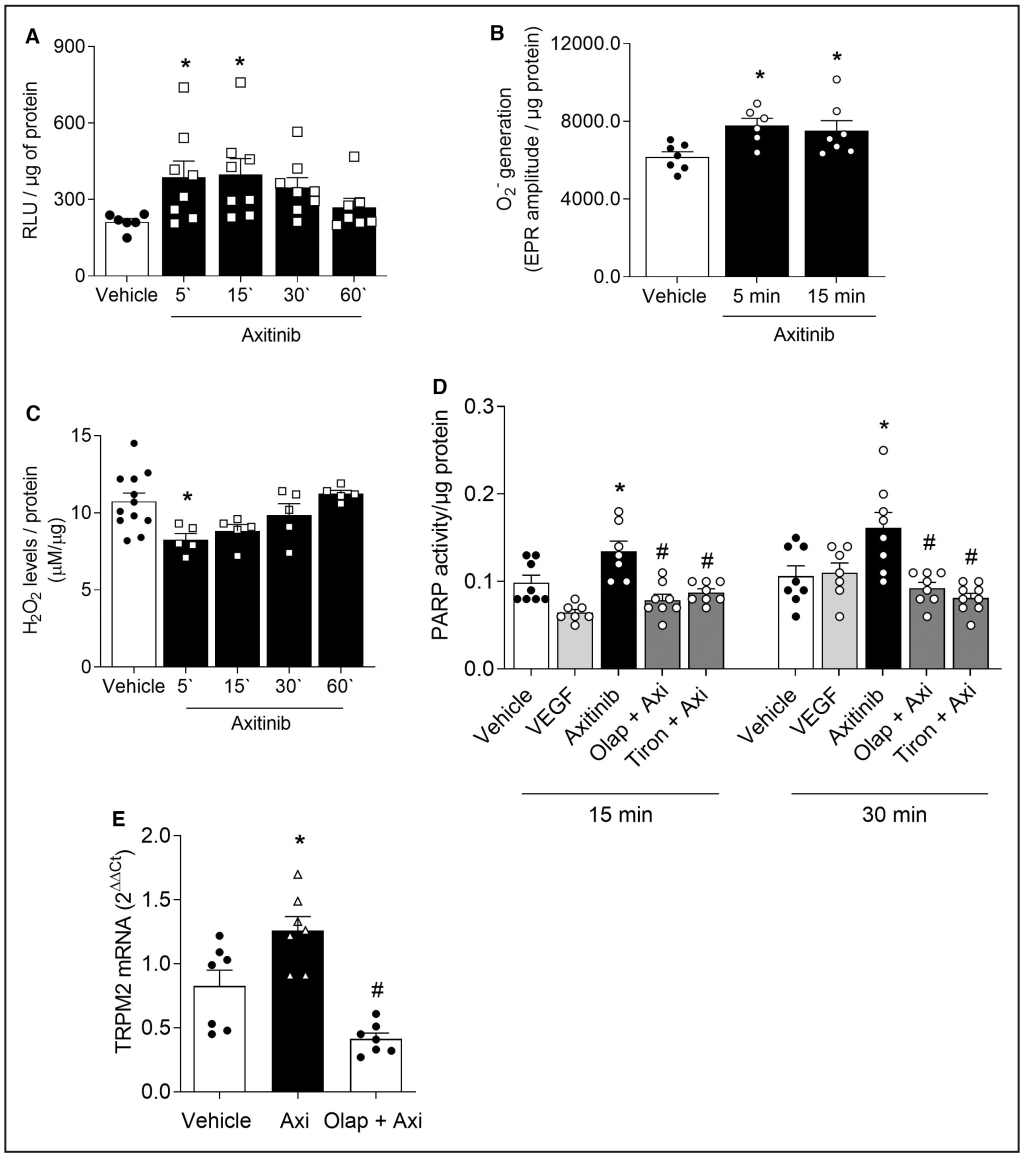

Figure 2. Axitinib increases poly (ADP-ribose) polymerase (PARP) activity and transient receptor potential cation channel, subfamily M, member 2 (TRPM2) expression in human vascular smooth muscle cells (VSMCs) in a reactive oxygen species (ROS)-dependent manner.
NADPH-dependent reactive oxygen species (ROS) production measured by lucigenin (**A**), electron paramagnetic resonance (superoxide) (**B**), and amplex red (H_2O_2) (**C**) in human VSMCs (n=5–9/group; 1-way ANOVA with Dunnett posttest; *P<0.05 axtinib vs vehicle). **D**, PARP activity was measured by colorimetric assay in human VSMCs in the absence and presence of olaparib and tiron (n=7–8/group; 1-way ANOVA with Dunnett post-test). Results are normalized by protein content (*P<0.05 axtinib vs vehicle, # Olap+Axi and Tiron+Axi vs axitinib). **E**, *TRPM2* gene expression in human VSMCs performed by real-time polymerase chain reaction. Gene expression was normalized to GAPDH (n=7/group; 1-way ANOVA with Dunnett posttest; *P<0.05 axtinib vs vehicle, # Olap+Axi vs axitinib). Results are expressed as mean±SEM.

PARP Inhibition Increases NOS Phosphorylation and NO Production in Endothelial Cells

The beneficial effects of PARP inhibition in endothelial dysfunction induced by axitinib was associated with eNOS/NO signaling. As demonstrated in Figure 5, when endothelial cells were exposed to the combination olaparib with axitinib, NO levels were similar to levels observed in VEGF-stimulated cells (Figure 5A). Additionally, the combination olaparib with axitinib reduced axitinib-induced eNOS Thr^{495} phosphorylation in endothelial cells (P<0.05; Figure 5B). No changes were observed in the activator site of eNOS Ser^{1177} (Figure S6).

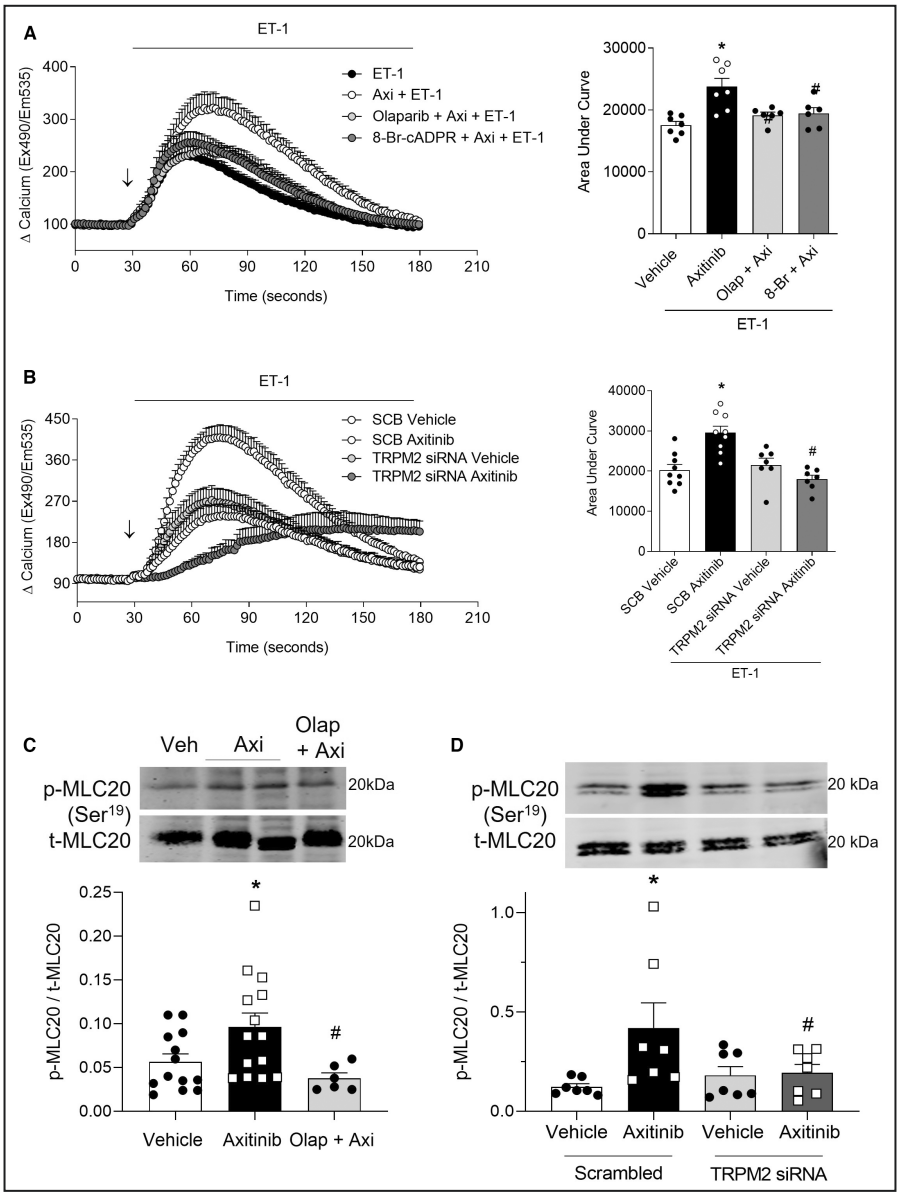

Figure 3. Increased intracellular free Ca^{2+} concentration $[Ca^{2+}]_i$ transients induced by axitinib in VSMCs are associated with poly (ADP-ribose) polymerase (PARP)–transient receptor potential cation channel, subfamily M, member 2 (TRPM2) activation.
A, Calcium transients were measured by live cell fluorescence imaging using the fluoroprobe Cal-520 AM. Representative tracings of human vascular smooth muscle cell (VSMC) $[Ca^{2+}]_i$ responses to endothelin-1 (ET-1; 0.1 μmol/L) in the presence or absence of olaparib or 8-Br-cADPR (n=6–7/group; *P<0.05 axitinib vs vehicle, # Olap+Axi vs axitinib). **B**, Calcium transients were also measured in cells exposed to scrambled (SCB) or TRPM2 small interfering RNA (siRNA) (n=7–9/group, *P<0.05 SCB axitinib vs SCB vehicle, # TRPM2 siRNA vs SCB axitinib). Experiments were repeated with >30 cells studied/field. $[Ca^{2+}]_i$ was quantified as area under the curve (1-way ANOVA with Dunnett posttest). **C**, Upper panel: representative immunoblot for phosphorylation of myosin light chain (MLC; S^{20}; MLC20) in human VSMCs exposed to axitinib in presence or absence of olaparib (30 min). Lower panel: quantification of p-MLC20. Protein expression was normalized to total MLC20 (n=6–13/group; 1-way ANOVA with Dunnett posttest; *P<0.05 axitinib vs vehicle, # Olap+Axi vs axitinib). **D**, Upper panel: representative immunoblot for the phosphorylation of MLC20 in human VSMCs exposed to axitinib in the presence of scramble and TRPM2 siRNA. Lower panel: quantification of p-MLC20. Protein expression was normalized to t-MLC20 (n=7/group; 1-way ANOVA with Dunnett posttest; *P<0.05 SCB axitinib vs SCB vehicle, # TRPM2 siRNA vs SCB axitinib). Results are expressed as mean±SEM.

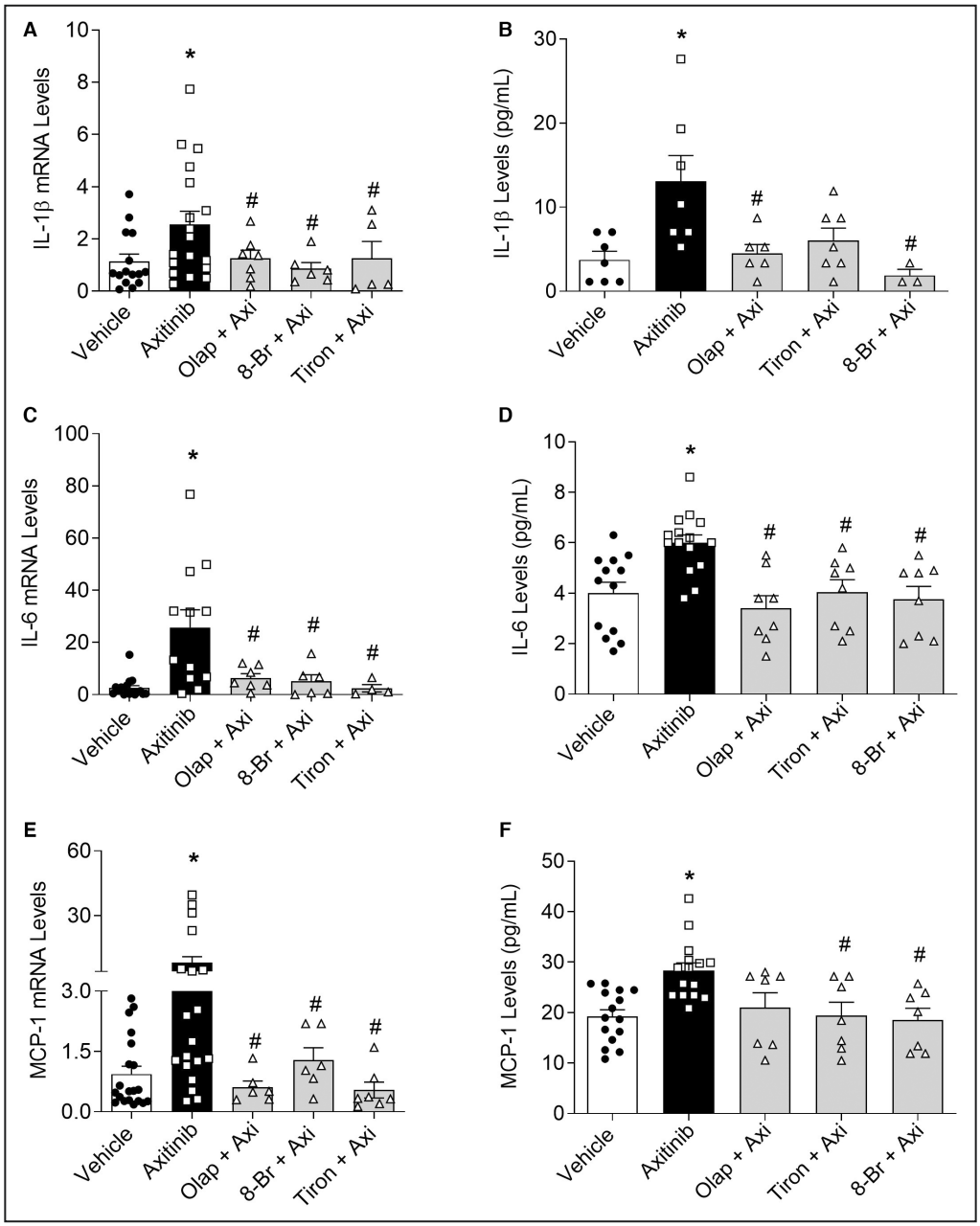

Figure 4. PARP inhibition ameliorates the increase in proinflammatory markers in human vascular smooth muscle cells (VSMCs) and VSMC media induced by axitinib.
Interleukin-1β (IL-1β) (**A**), Interleukin-6 (IL-6) (**C**), and monocyte chemoattractant protein-1 (MCP-1) (**E**) gene expression in human VSMCs. Analysis was performed by real-time polymerase chain reaction, and gene expression was normalized to GAPDH (n=4–18; 1-way ANOVA with Dunnett posttest). IL-1β (**B**), IL-6 (**D**), and MCP-1 (**F**) levels were detected in human VSMC media by ELISA assay (n=3–15/group; 1-way ANOVA with Dunnett posttest). Results are expressed as mean±SEM. *P<0.05 axitinib vs vehicle, # Olap+Axi, 8-Br+Axi or Tiron+Axi vs axitinib.

DISCUSSION

This study demonstrates a role for PARP and TRPM2 in vascular dysfunction induced by VEGF inhibition. This is supported by the findings that (1) VEGF inhibition is associated with oxidative stress, activation of PARP, and upregulation of redox-sensitive TRPM2; (2) olaparib and TRPM2 siRNA blunt axitinib-induced calcium influx and MLC20 phosphorylation, and attenuate proinflammatory responses in VSMC with improved eNOS-NO signaling in endothelial cells; and (3) ex vivo vascular studies showed that PARP and TRPM2 inhibition improve hypercontractile responses and endothelium-dependent dysfunction in arteries

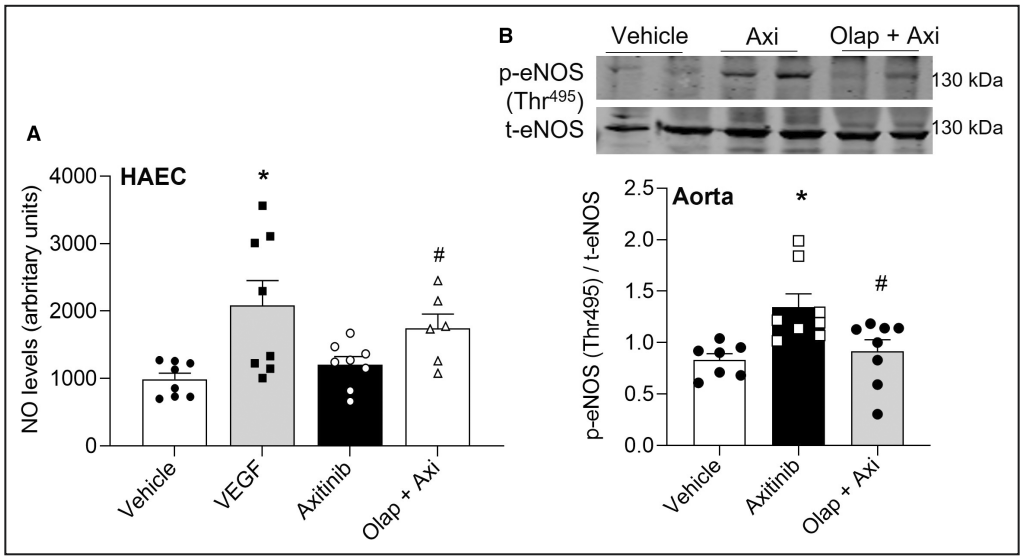

Figure 5. Axitinib reduces endothelial nitric oxide synthase (eNOS)/nitric oxide (NO) signaling in human aortic endothelial cells (HAECs), which is prevented by poly (ADP-ribose) polymerase (PARP) inhibition.

A, NO production was determined by diaminofluorescein-2 diacetate (DAF2-DA) fluorescence in HAECs exposed to axitinib in the presence or absence of olaparib (30 min). Values from DAF2-DA were normalized by protein amount (n=7–9; 1-way ANOVA with Dunnett posttest). **B**, Upper panel: representative immunoblot for the phosphorylation of eNOS (Thr^{495}) determined by immunoblotting in HAECs in the presence or absence of olaparib. Lower panel: quantification of phospho-eNOS. Protein expression was normalized to total eNOS (t-eNOS; n=6–8/group; 1-way ANOVA with Dunnett posttest). Results represent the mean±SEM. *P<0.05 axitinib vs vehicle, # Olap+Axi vs axitinib.

exposed to axitinib. Collectively, these findings suggest that PARP inhibition attenuates VEGFi-induced VSMC oxidative stress and inflammation and vascular dysfunction, processes important in the pathophysiology of hypertension. Our findings may explain, in part, the clinical observations that hypertension in patients treated with combination olaparib and bevacizumab is lower than with bevacizumab monotherapy.[8]

We previously demonstrated that VEGF inhibition increases ROS production in different vascular beds, vascular cells, and organs.[16,19,22] Here, we advance these findings and show that VEGFi-induced oxidative stress is associated with PARP activation. ROS is a potent stimulus for PARP activation and DNA damage. Oxidative stress–induced overactivation of PARP-1 consumes nicotinamide adenine dinucleotide and consequently ATP, resulting in cellular dysfunction and cell death.[23,24] PARP-1 also interacts with proinflammatory transcription factors, including NF-κB, increasing proinflammatory mediators. These PARP-mediated phenomena are especially relevant in cardiovascular diseases, which are characterized by oxidative stress and vascular inflammation such as heart failure, hypertensive organ damage, stroke, and myocardial infarction.[25] Preclinical studies demonstrated beneficial effects of PARPis in these conditions.[12,26] Of significance, Ca^{2+} is coupled to PARP-1 through Ca^{2+} channels, especially TRPM2,[27] which we show is regulated by axitinib.

TRPM2 is a highly redox-sensitive Ca^{2+} and Na^{+} channel. Vascular injury and DNA damage lead to rapid recruitment of PARP-1 to sites of damage, resulting in the polymerization of ADP-ribose, which in turn activates TRPM2, leading to increased Ca^{2+} influx.[12,26] This was demonstrated in human cells and experimental models highlighting an important role for redox-regulated PARP-TRPM2 modulation of Ca^{2+}, which contributes to vascular hypercontractility in hypertension.[12] These findings are in accordance with our data showing that PARP and TRPM2 inhibition attenuate vascular and endothelial dysfunction induced by VEGF inhibition. Additionally, olaparib and downregulation of TRMP2 reduced Ca^{2+} influx and phosphorylation of contractile proteins (MLC20) induced by axitinib. Changes in Ca^{2+} dynamics have also been shown for ibrutinib, another tyrosine kinase inhibitor, in spontaneously hypertensive rats.[28]

Previous studies showed that VEGF inhibition is associated with reduced NO production, which has been implicated in blood pressure elevation during VEGF inhibition.[16,29] In our experiments, we observed endothelial dysfunction in small resistance arteries exposed to axitinib, which was attenuated by PARP and TRPM2 inhibition, with no changes in endothelium-independent

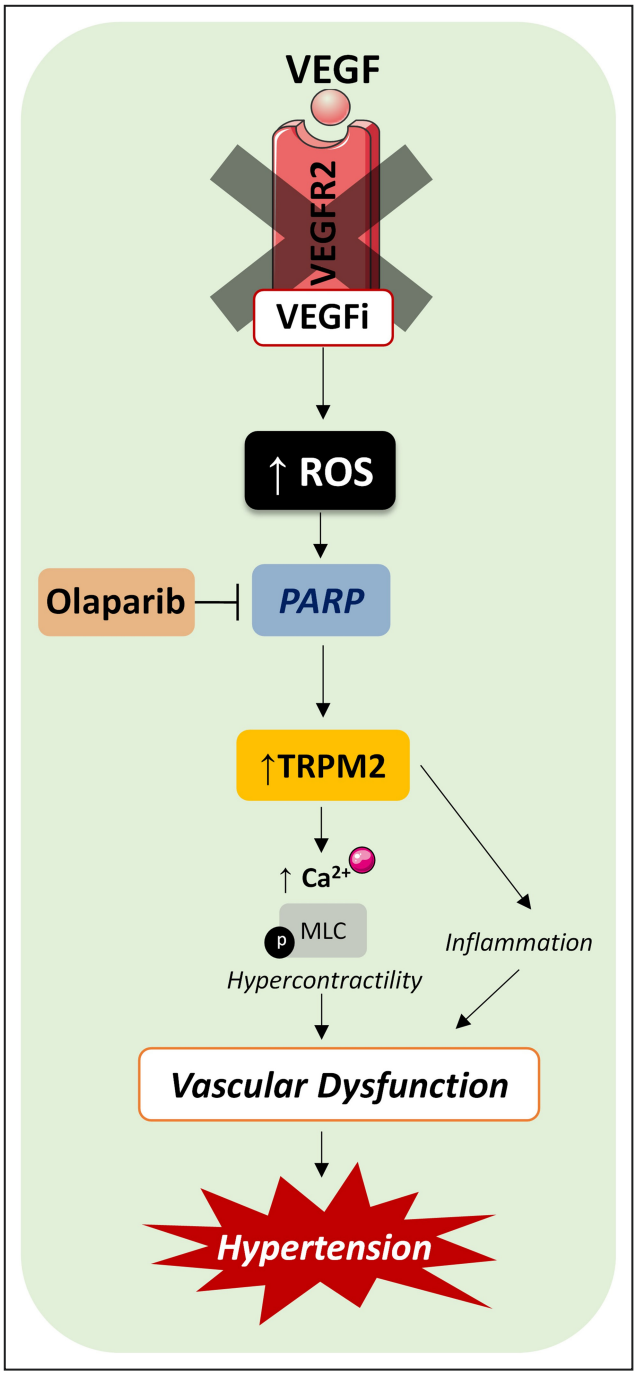

Figure 6. Schematic showing possible mechanisms underlying vascular dysfunction associated with vascular endothelial growth factor (VEGF) inhibition and the role of poly (ADP-ribose) polymerase (PARP)–transient receptor potential cation channel, subfamily M, member 2 (TRPM2) axis.
We demonstrated that axitinib increases ROS production in human vascular smooth muscle cells (VSMCs), which is associated with activation of the PARP-TRPM2 axis. Enhanced PARP-TRPM2 signaling causes an increase in calcium (Ca^{2+}) influx and procontractile signaling, leading to VSMC hypercontractility, as well as an increase in inflammatory responses. PARP inhibition attenuated VEGF inhibitor (VEGFi)-induced effects. Together this suggests that VEGF inhibition induces vascular dysfunction and proinflammatory responses via PARP-TRPM2 activation. Inhibition of PARP-TRPM2 signaling may represent an efficient approach to ameliorate vascular toxicity induced by VEGFi in patients with cancer. This may be clinically relevant because combination PARP and VEGF inhibitors are increasingly being used to treat some cancers. MLC indicates myosin light chain; and ROS, reactive oxygen species.

responses. We previously reported that 2-week treatment with the VEGF inhibitor vatalanib induced endothelial dysfunction in mice.[16] In the present study, we showed that axitinib decreases NO signaling in human endothelial cells, effects that are reversed by olaparib. This is further corroborated by others showing that PARP inhibition improves hyperhomocysteinemia-[30] and age-dependent endothelial dysfunction[31] by regulating NO bioavailability. PARP-1 inhibition was also shown to improve endothelial function by enhancing VEGFR2/Akt/BAD phosphorylation, and by reducing inflammation via NF-κB.[32]

Increased proinflammatory responses in VSMCs treated with axitinib confirmed our previous observations in endothelial cells exposed to microparticles from VEGFi-treated patients with cancer.[19] This has pathophysiological significance because inflammation has been implicated in the development of hypertension.[25] The increase in cytokines and chemokines was attenuated by PARP and TRPM2 inhibition and by a ROS scavenger, which reiterates the role of ROS-PARP-TRPM2 in vascular dysfunction induced by VEGF inhibition. Similar findings were recently demonstrated in renal ischemia–reperfusion injury, where PARP inhibition diminished inflammatory cell infiltration and proinflammatory cytokine/chemokine expressions in postischemic kidneys.[33] TRPM2 has also been linked to inflammatory responses. Recent studies showed that TRPM2 mediates inflammasome activation in immune cells.[34] Knockout or inhibition of TRPM2 blocked ROS-dependent NLRP3 inflammasome activation in macrophages.[11] Products of inflammasome enhance peripheral organ inflammation and exacerbate hypertension by acting on innate immune cells and T cells directly.[35] TRPM2 is also associated with exacerbated systemic immune responses in ischemic stroke,[10] inflammation-associated endothelial cell death, and permeability disruption.[13]

Our findings have potential clinical significance. Not only do we identify PARP/TRPM2 as a novel molecular pathway underlying VEGFi-induced VSMC toxicity, but we provide some molecular insights how PARP inhibition may attenuate blood pressure elevation caused by VEGFis in patients with cancer. PARPis have transformed ovarian cancer treatment,[6,36] and more recently have also been approved for the treatment of metastatic castration-resistant prostate cancer.[37] The use of PARPis following chemotherapy has become the standard of care in some cancers. The combination of PARPis with antiangiogenic

agents has demonstrated synergistic activity in clinical studies. The PAOLA-1/ENGOT-ov25 clinical trial (NTC02477644) showed that in patients with advanced ovarian cancer receiving bevacizumab, the addition of olaparib provided a substantial survival benefit. In addition, the increase in blood pressure observed in patients treated with bevacizumab was less in patients receiving combination bevacizumab plus olaparib. More specifically, 46% and 19% of patients treated with the combination showed all grades and grade ≥3, respectively, versus 60% and 30% of patients treated only with bevacizumab.[8] These data suggest that olaparib may lower the risk of hypertension in patients with cancer treated with antiangiogenic drugs, through undefined mechanisms. Our data shed some light on potential mechanisms since PARP is involved in VEGFi-induced VSMC dysfunction, effects that are ameliorated by PARP inhibition. Further studies are warranted to better understand the potential vasoprotective effect of combination PARP-VEGF inhibition in the treatment of cancer.

In conclusion, our study defines a novel mechanism underlying VEGFi-induced vascular damage by highlighting the importance of PARP and TRPM2. Increased generation of ROS and oxidative stress in VEGFi-treated VSMCs likely promotes activation of PARP and TRPM2, which in turn increases procontractile and proinflammatory signaling and consequent vascular dysfunction (Figure 6). In the context of cancer treatment, combination therapy with olaparib and VEGFi may attenuate vascular toxicity associated with VEGF inhibition, while at the same time may provide added anticancer benefit. This awaits clarification in clinical studies.

CONCLUSIONS

Our data indicate that PARP/TRPM2 inhibition attenuates axitinib-mediated vascular dysfunction and normalizes impaired human VSMCs and endothelial cell signaling induced by VEGFis.

ARTICLE INFORMATION

Received August 9, 2022; accepted January 12, 2023.

Affiliations

Institute of Cardiovascular and Medical Sciences, University of Glasgow, Glasgow, United Kingdom (K.B.N., R.A., A.C.M., R.M.T.); Strathclyde Institute of Pharmacy and Biomedical Sciences, University of Strathclyde, Glasgow, United Kingdom (K.B.N.); and Research Institute of the McGill University Health Centre (RI-MUHC), McGill University, Montreal, Canada (A.C.M., R.M.T.).

Acknowledgments

The authors thank Wendy Beattie for help with the human cells and mouse colonies, Laura Haddow and John McAbeny for technical support in the myography facility, and the BHF Myography & Imaging Core Facility. Prof Ninian Lang is thanked for useful discussion.

Sources of Funding

This study was supported by grants from the British Heart Foundation (BHF; RE/13/5/30177; 18/6/34217; CH/12/29762). Dr Montezano was supported through a Walton Foundation fellowship, University of Glasgow. Dr Touyz is supported by grants from the Leducq Foundation, Dr. Phil Gold Chair, McGill University, and the European Commission.

Disclosures

None.

Supplemental Material

Table S1
Figures S1–S6

REFERENCES

1. van Dorst DCH, Dobbin SJH, Neves KB, Herrmann J, Herrmann SM, Versmissen J, Mathijssen RHJ, Danser AHJ, Lang NN. Hypertension and prohypertensive antineoplastic therapies in cancer patients. *Circ Res*. 2021;128:1040–1061. doi: 10.1161/CIRCRESAHA.121.318051
2. Herrmann J. Vascular toxic effects of cancer therapies. *Nat Rev Cardiol*. 2020;17:503–522. doi: 10.1038/s41569-020-0347-2
3. Dobbin SJH, Petrie MC, Myles RC, Touyz RM, Lang NN. Cardiotoxic effects of angiogenesis inhibitors. *Clin Sci (Lond)*. 2021;135:71–100. doi: 10.1042/CS20200305
4. Small HY, Montezano AC, Rios FJ, Savoia C, Touyz RM. Hypertension due to antiangiogenic cancer therapy with vascular endothelial growth factor inhibitors: understanding and managing a new syndrome. *Can J Cardiol*. 2014;30:534–543. doi: 10.1016/j.cjca.2014.02.011
5. Zamorano JL, Lancellotti P, Rodriguez Munoz D, Aboyans V, Asteggiano R, Galderisi M, Habib G, Lenihan DJ, Lip GYH, Lyon AR, et al. 2016 ESC position paper on cancer treatments and cardiovascular toxicity developed under the auspices of the ESC Committee for Practice Guidelines: the Task Force for cancer treatments and cardiovascular toxicity of the European Society of Cardiology (ESC). *Eur J Heart Fail*. 2017;19:9–42. doi: 10.1002/ejhf.654
6. Boussios S, Karihtala P, Moschetta M, Karathanasi A, Sadauskaite A, Rassy E, Pavlidis N. Combined strategies with poly (ADP-ribose) polymerase (PARP) inhibitors for the treatment of ovarian cancer: a literature review. *Diagnostics (Basel)*. 2019;9:9. doi: 10.3390/diagnostics9030087
7. Rose M, Burgess JT, O'Byrne K, Richard DJ, Bolderson E. PARP inhibitors: clinical relevance, mechanisms of action and tumor resistance. *Front Cell Dev Biol*. 2020;8:564601. doi: 10.3389/fcell.2020.564601
8. Ray-Coquard I, Pautier P, Pignata S, Pérol D, González-Martín A, Berger R, Fujiwara K, Vergote I, Colombo N, Mäenpää J, et al. Olaparib plus bevacizumab as first-line maintenance in ovarian cancer. *N Engl J Med*. 2019;381:2416–2428. doi: 10.1056/NEJMoa1911361
9. Naziroglu M. New molecular mechanisms on the activation of TRPM2 channels by oxidative stress and ADP-ribose. *Neurochem Res*. 2007;32:1990–2001. doi: 10.1007/s11064-007-9386-x
10. Wang Q, Liu N, Ni YS, Yang JM, Ma L, Lan XB, Wu J, Niu JG, Yu JQ. TRPM2 in ischemic stroke: structure, molecular mechanisms, and drug intervention. *Channels (Austin)*. 2021;15:136–154. doi: 10.1080/19336950.2020.1870088
11. Zhong Z, Zhai Y, Liang S, Mori Y, Han R, Sutterwala FS, Qiao L. TRPM2 links oxidative stress to NLRP3 inflammasome activation. *Nat Commun*. 2013;4:1611. doi: 10.1038/ncomms2608
12. Alves-Lopes R, Neves KB, Anagnostopoulou A, Rios FJ, Lacchini S, Montezano AC, Touyz RM. Crosstalk between vascular redox and calcium signaling in hypertension involves TRPM2 (transient receptor potential melastatin 2) cation channel. *Hypertension*. 2020;75:139–149. doi: 10.1161/HYPERTENSIONAHA.119.13861
13. Zielinska W, Zabrzynski J, Gagat M, Grzanka A. The role of TRPM2 in endothelial function and dysfunction. *Int J Mol Sci*. 2021;22. doi: 10.3390/ijms22147635
14. Jagtap P, Szabo C. Poly(ADP-ribose) polymerase and the therapeutic effects of its inhibitors. *Nat Rev Drug Discov*. 2005;4:421–440. doi: 10.1038/nrd1718
15. Pacher P, Szabo C. Role of the peroxynitrite-poly(ADP-ribose) polymerase pathway in human disease. *Am J Pathol*. 2008;173:2–13. doi: 10.2353/ajpath.2008.080019
16. Neves KB, Rios FJ, van der Mey L, Alves-Lopes R, Cameron AC, Volpe M, Montezano AC, Savoia C, Touyz RM. VEGFR (vascular endothelial

growth factor receptor) inhibition induces cardiovascular damage via redox-sensitive processes. *Hypertension*. 2018;71:638–647. doi: 10.1161/HYPERTENSIONAHA.117.10490
17. Montezano AC, Lopes RA, Neves KB, Rios F, Touyz RM. Isolation and culture of vascular smooth muscle cells from small and large vessels. *Methods Mol Biol*. 2017;1527:349–354. doi: 10.1007/978-1-4939-6625-7_27
18. Lopes RA, Neves KB, Tostes RC, Montezano AC, Touyz RM. Downregulation of nuclear factor erythroid 2-related factor and associated antioxidant genes contributes to redox-sensitive vascular dysfunction in hypertension. *Hypertension*. 2015;66:1240–1250. doi: 10.1161/HYPERTENSIONAHA.115.06163
19. Neves KB, Rios FJ, Jones R, Jeffry Evans TR, Montezano AC, Touyz RM. Microparticles from VEGF inhibitor-treated cancer patients mediate endothelial cell injury. *Cardiovasc Res*. 2019;115:978–988. doi: 10.1093/cvr/cvz021
20. Touyz RM, Alves-Lopes R, Rios FJ, Camargo LL, Anagnostopoulou A, Arner A, Montezano AC. Vascular smooth muscle contraction in hypertension. *Cardiovasc Res*. 2018;114:529–539. doi: 10.1093/cvr/cvy023
21. Knowles H, Li Y, Perraud AL. The TRPM2 ion channel, an oxidative stress and metabolic sensor regulating innate immunity and inflammation. *Immunol Res*. 2013;55:241–248. doi: 10.1007/s12026-012-8373-8
22. Cameron AC, Welsh P, Neves KB, Newby DE, Touyz RM, Lang NN. Acute vascular effects of vascular endothelial growth factor inhibition in the forearm arterial circulation. *J Hypertens*. 2020;38:257–265. doi: 10.1097/HJH.0000000000002230
23. Luo X, Kraus WL. On PAR with PARP: cellular stress signaling through poly(ADP-ribose) and PARP-1. *Genes Dev*. 2012;26:417–432. doi: 10.1101/gad.183509.111
24. Alves-Lopes R, Touyz RM. PARP-1 (poly[ADP-ribose] polymerase-1). *Hypertension*. 2018;72:1087–1089. doi: 10.1161/HYPERTENSIONAHA.118.11830
25. Guzik TJ, Touyz RM. Oxidative stress, inflammation, and vascular aging in hypertension. *Hypertension*. 2017;70:660–667. doi: 10.1161/HYPERTENSIONAHA.117.07802
26. Henning RJ, Bourgeois M, Harbison RD. Poly(ADP-ribose) polymerase (PARP) and PARP inhibitors: mechanisms of action and role in cardiovascular disorders. *Cardiovasc Toxicol*. 2018;18:493–506. doi: 10.1007/s12012-018-9462-2
27. Yu P, Xue X, Zhang J, Hu X, Wu Y, Jiang LH, Jin H, Luo J, Zhang L, Liu Z, et al. Identification of the ADPR binding pocket in the NUDT9 homology domain of TRPM2. *J Gen Physiol*. 2017;149:219–235. doi: 10.1085/jgp.201611675
28. Du B, Chakraborty P, Azam MA, Massé S, Lai PFH, Niri A, Si D, Thavendiranathan P, Abdel-Qadir H, Billia F, et al. Acute effects of ibrutinib on ventricular arrhythmia in spontaneously hypertensive rats. *JACC CardioOncol*. 2020;2:614–629. doi: 10.1016/j.jaccao.2020.08.012
29. Lankhorst S, Kappers MH, van Esch JH, Danser AH, van den Meiracker AH. Hypertension during vascular endothelial growth factor inhibition: focus on nitric oxide, endothelin-1, and oxidative stress. *Antioxid Redox Signal*. 2014;20:135–145. doi: 10.1089/ars.2013.5244
30. Yu X, Cheng X, Xie JJ, Yao R, Chen Y, Ding YJ, Tang TT, Liao YH. Poly (ADP-ribose) polymerase inhibition improves endothelial dysfunction induced by hyperhomocysteinemia in rats. *Cardiovasc Drugs Ther*. 2009;23:121–127. doi: 10.1007/s10557-008-6146-3
31. Zhang GH, Chao M, Hui LH, Xu DL, Cai WL, Zheng J, Gao M, Zhang MX, Wang J, Lu QH. Poly(ADP-ribose)polymerase 1 inhibition protects against age-dependent endothelial dysfunction. *Clin Exp Pharmacol Physiol*. 2015;42:1266–1274. doi: 10.1111/1440-1681.12484
32. Mathews MT, Berk BC. PARP-1 inhibition prevents oxidative and nitrosative stress-induced endothelial cell death via transactivation of the VEGF receptor 2. *Arterioscler Thromb Vasc Biol*. 2008;28:711–717. doi: 10.1161/ATVBAHA.107.156406
33. Jang HR, Lee K, Jeon J, Kim JR, Lee JE, Kwon GY, Kim YG, Kim DJ, Ko JW, Huh W. Poly (ADP-ribose) polymerase inhibitor treatment as a novel therapy attenuating renal ischemia-reperfusion injury. *Front Immunol*. 2020;11:564288. doi: 10.3389/fimmu.2020.564288
34. Wang L, Negro R, Wu H. TRPM2, linking oxidative stress and Ca(2+) permeation to NLRP3 inflammasome activation. *Curr Opin Immunol*. 2020;62:131–135. doi: 10.1016/j.coi.2020.01.005
35. Patrick DM, Van Beusecum JP, Kirabo A. The role of inflammation in hypertension: novel concepts. *Curr Opin Physiol*. 2021;19:92–98. doi: 10.1016/j.cophys.2020.09.016
36. Coleman RL, Fleming GF, Brady MF, Swisher EM, Steffensen KD, Friedlander M, Okamoto A, Moore KN, Ben-Baruch NE, Werner TL, et al. Veliparib with first-line chemotherapy and as maintenance therapy in ovarian cancer. *N Engl J Med*. 2019;381:2403–2415. doi: 10.1056/NEJMoa1909707
37. de Bono J, Mateo J, Fizazi K, Saad F, Shore N, Sandhu S, Chi KN, Sartor O, Agarwal N, Olmos D, et al. Olaparib for metastatic castration-resistant prostate cancer. *N Engl J Med*. 2020;382:2091–2102. doi: 10.1056/NEJMoa1911440

SUPPLEMENTAL MATERIAL

Table S1. Human primers used in the study.

Primer	Sense primer	Anti-sense primer
GAPDH	GAGTCAACGGATTTGGTCGT	TTGATTTTGGAGGGATCTCG
TRPM2	TTCGTGGATTCCTGAAAACATCA	GTCTGCTCCGATATGAACTTCTC
iNOS	ACAAGCCTACCCCTCCAGAT	TCCCGTCAGTTGGTAGGTTC
MCP-1	CCCCAGTCACCTGCTGTTAT	AGATCTCCTTGGCCACAATG
IL-6	AGGAGACTTGCCTGGTGAAA	CAGGGGTGGTTATTGCATCT
IL-1β	CTGTCCTGCGTGTTGAAAGAT	TTCTGCTTGAGAGGTGCTGAT

Figure S1. Effects of niraparib on vascular reactivity.

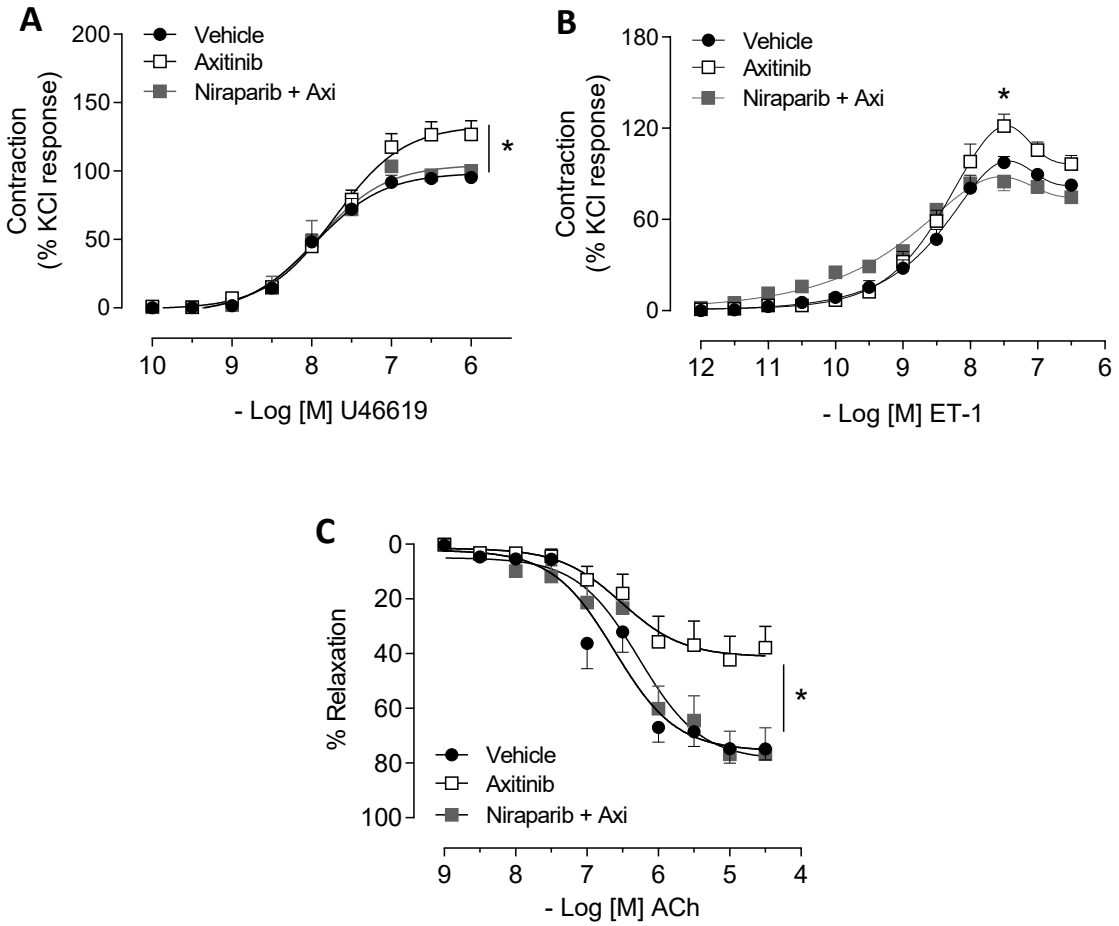

Vascular functional responses in mesenteric arteries obtained from FVB mice in response to (A) U46619, (B) endothelin-1 (ET-1) and (C) acetylcholine (ACh). Function was assessed by wire myography. The increase in contraction and impaired relaxation induced by axitinib was also ameliorated in vessels pre-treated with the PARP inhibitor niraparib (A, B, C) (n= 4-7/group). Curves represent the mean±SEM. For ACh, responses were expressed as percentage of U46619-induced pre-constriction. Non-parametric test Kruska-Wallis. *p<0.05 *vs.* vehicle, # *vs.* Axitinib.

Figure S2. Increased $[Ca^{2+}]_i$ transients induced by axitinib in human VSMC are associated with PARP-TRPM2 activation.

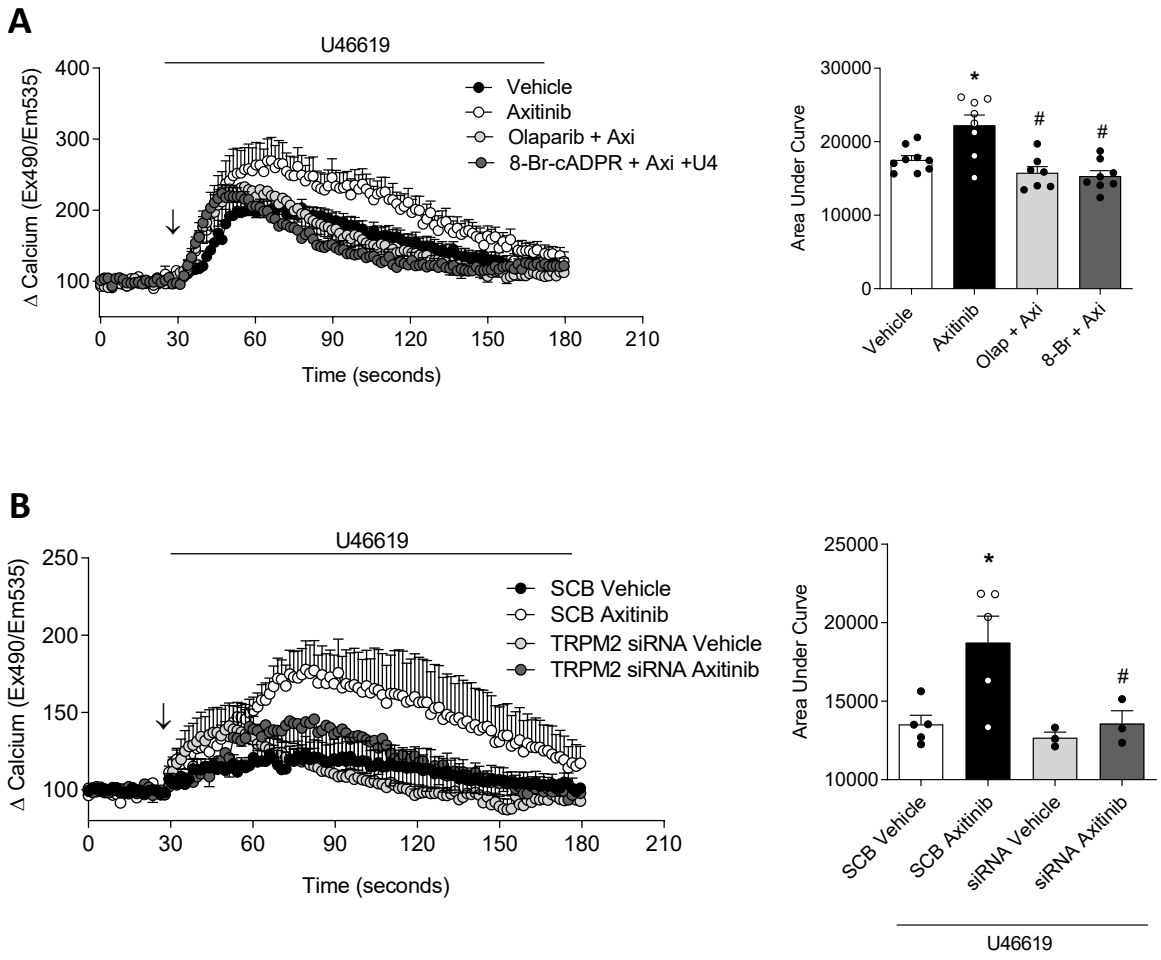

(A) Calcium transients were measured by live cell fluorescence imaging using the fluoroprobe Cal-520 AM. Representative tracings of VSMC $[Ca^{2+}]_i$ responses to U46619 (1 μmol/L) in human VSMC in presence or absence of olaparib or 8-Br-cADPR (n=7-8/group). (B) Calcium transients were also measured in cells exposed to TRPM2 siRNA (n=3-5/group). Experiments were repeated with >30 cells studied/field. $[Ca^{2+}]_i$ was quantified as area under the curve (One-way ANOVA with Dunnett post-test). *p<0.05 *vs.* vehicle, # *vs.* Axitinib.

Figure S3. ROS scavenger and PARP inhibitor decrease phosphorylation of contractile markers in human VSMC, and aorta exposed to axitinib.

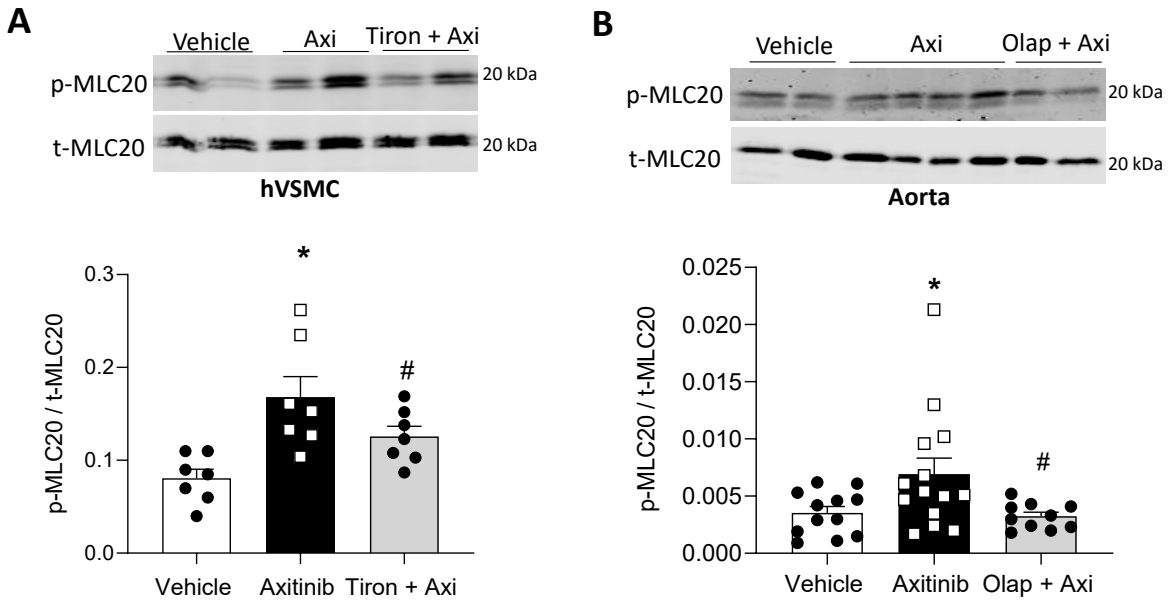

(A) Upper panel: representative immunoblot for the phosphorylation of myosin light chain (S^{20}) in human VSMC exposed to axitinib in presence or absence of tiron (ROS scavenger; 30 minutes); Lower panels: quantification of p-MLC20. Protein expression was normalised to t-MLC20 (n=7; One-way ANOVA with Dunnett post-test). (B) Upper panel: representative immunoblot for the phosphorylation of myosin light chain in aortas from control mice exposed to axitinib for 24 hours in presence or absence of olaparib (PARP inhibitor; 30 minutes); Lower panels: quantification of p-MLC20. Protein expression was normalised to t-MLC20 (n=10-15/group; One-way ANOVA with Dunnett post-test). Results are expressed as mean±SEM. *p<0.05 *vs.* vehicle, # *vs.* Axitinib.

Figure S4. PARP inhibition ameliorates the increase of iNOS mRNA levels in human VSMC induced by axitinib.

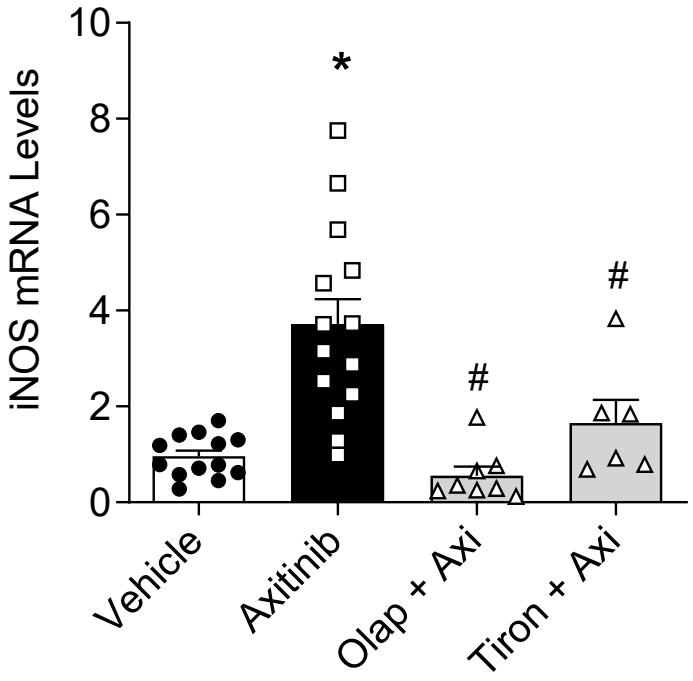

iNOS gene expression in human VSMC. Analysis was performed by qPCR and gene expression was normalised to GAPDH (n=6-14/group); One-way ANOVA with Dunnett post-test). Results are expressed as mean±SEM. *p<0.05 Axitinib *vs.* vehicle, # Olap + Axi *vs.* Axitinib.

Figure S5. PARP inhibition ameliorates the increase of NFkB protein expression in human VSMC induced by axitinib.

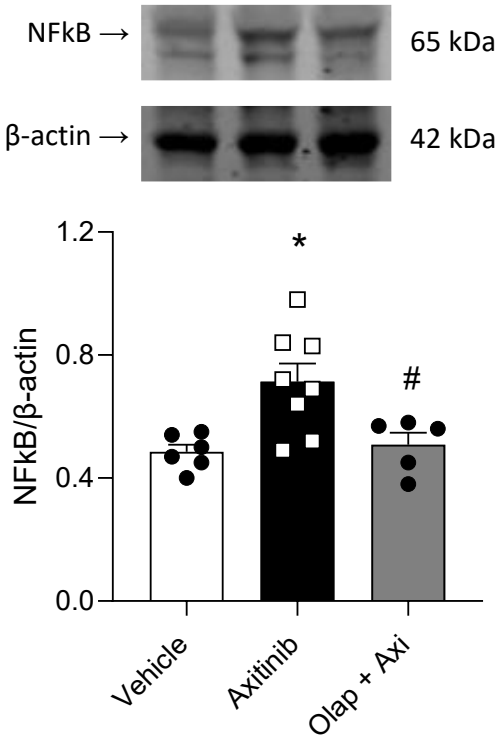

(A) Upper panel: representative immunoblot for NFkB protein expression in hVSMC exposed to axitinib for 15 minutes in presence or absence of olaparib (PARP inhibitor; 30 minutes); Lower panels: quantification of β-actin. Protein expression was normalised to β-actin (n=5-8/group; One-way ANOVA with Dunnett post-test). Results are expressed as mean±SEM. *p<0.05 Axitinib *vs.* vehicle, # Olap + Axi *vs.* Axitinib.

Figure S6. Axitinib does not change the phosphorylation of the activator site of eNOS in aorta.

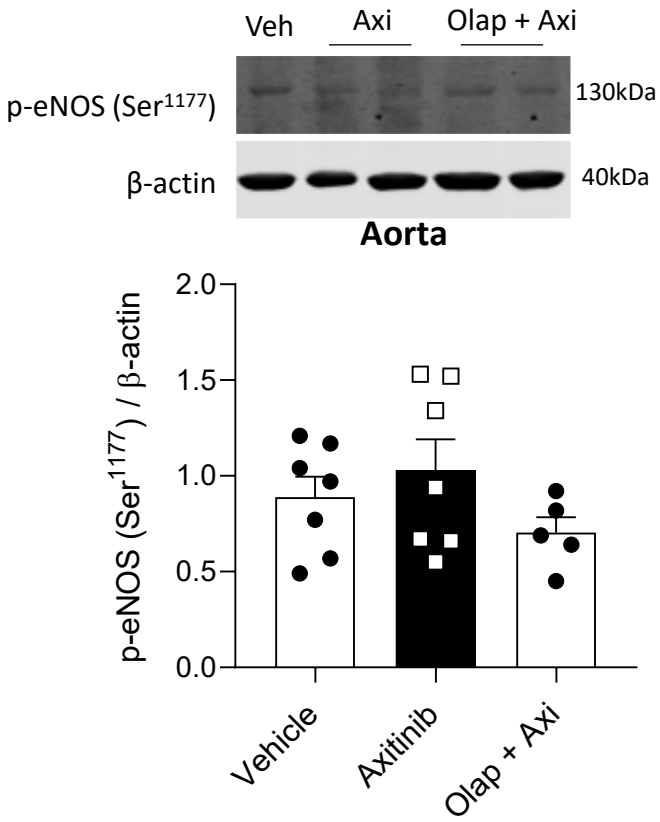

(A) Upper panel: representative immunoblot for the phosphorylation of eNOS (Ser^{1177}) in aortas from control mice exposed to axitinib for 24 hours in presence or absence of olaparib (PARP inhibitor; 30 minutes); Lower panels: quantification of p-eNOS. Protein expression was normalised to t-eNOS (n=5-7/group; One-way ANOVA with Dunnett post-test). Results are expressed as mean±SEM.